Int. J. Heat Mass Transfer. Vol. 32, No. 9, pp. 1619–1630, 1989
Printed in Great Britain

0017–9310/89 $3.00 + 0.00

Augmented heat transfer in rectangular channels of narrow aspect ratios with rib turbulators

J. C. HAN, S. OU, J. S. PARK and C. K. LEI
Department of Mechanical Engineering, Texas A&M University, College Station, TX 77843-3123, U.S.A.

(*Received* 23 *May* 1988 *and in final form* 3 *January* 1989)

Abstract—The effects of the rib angle-of-attack on the distributions of the local heat transfer coefficient and on the friction factors in short rectangular channels of narrow aspect ratios with a pair of opposite rib-roughened walls are determined for Reynolds numbers from 10 000 to 60 000. The channel width-to-height ratios are 2/4 and 1/4; the corresponding rib angles-of-attack are 90°, 60°, 45°, and 30°, respectively. The results indicate that the narrow-aspect-ratio channels give better heat transfer performance than the wide-aspect-ratio channels for a constant pumping power. Semi-empirical friction and heat transfer correlations are obtained. The results can be used in the design of turbine cooling channels of narrow aspect ratios.

INTRODUCTION

FOR HIGH thermal efficiency and high power density, the trend in advanced aeroengine design is toward high entry gas temperature (1400–1500°C), well above the allowable metal temperature. Therefore, highly sophisticated, efficient, cooling technologies such as film cooling, impingement cooling, and rib/pin augmented cooling are employed for vanes and blades of advanced gas turbines. This investigation focuses on the augmented heat transfer in turbine cooling channels with rib turbulators. Figure 1(a) is a cross-sectional view of an internally-cooled turbine blade. Since heat is conducted from the pressure and suction surfaces, turbulence promotors (rib turbulators) are cast only on two opposite walls of the cooling channels (i.e. inner walls of the pressure and suction surface) to enhance heat transfer to the cooling air. The cross sections of the cooling channels are nearly rectangular and have a range of channel aspect ratios. Because of the blade shape, cooling channels near the trailing edge have broad aspect ratios ($W/H \geqslant 1$) and those near the leading edge have narrow aspect ratios ($W/H \leqslant 1$), as shown in Fig. 1(a). References [1, 2] investigated systematically the effects of rib configurations (such as rib height, spacing, angle of attack) and flow Reynolds numbers on the average heat transfer and pressure drop in the fully developed region of a uniformly heated, square channel ($W/H = 1$) with two opposite rib-roughened walls. References [3, 4] reported the effects of the above parameters on the local heat transfer and pressure drop in developing (entrance) and fully developed regions of foil-heated, rectangular channels with large aspect ratios ($W/H = 1$, 2, and 4) with two opposite rib-roughened walls. The results [1–4] show that, in the square channel, the highest heat transfer coefficient, accompanied by the highest friction factor, was at rib angles-of-attack between 60° and 75°; the best heat transfer performance for a constant pumping power was at rib angles-of-attack between 30° and 45°. The results also show that the square channel ($W/H = 1$) gives a better heat transfer performance than the rectangular channels of large aspect ratios ($W/H = 2$ and 4) in which heat transfer performance is insensitive to the rib angle-of-attack. These results are obtained primarily for short rectangular channels ($L/D = 10$–15) with large aspect ratios ($W/H = 1$, 2, and 4, ribs on side W) and with parallel ribs (the ribs on two opposite walls of the cooling channels are in parallel orientations). It is of interest whether the results [3, 4] obtained for short rectangular channels with large aspect ratios ($W/H > 1$) can be applied to short rectangular channels with small aspect ratios ($W/H < 1$) in cooling channels close to the leading edge of the turbine blade. It is questionable whether the crossed ribs (the ribs on two opposite walls of the cooling channels are in the crossed orientations), as shown in Fig. 1(b), can provide a better heat transfer performance than the parallel ribs used in refs. [3, 4]. Furthermore, for turbine cooling design, it is important to know the distributions of the local heat transfer coefficient for developing flow in short rectangular channels with rib turbulators. Thus further investigation was needed to determine the effect of the rib angle-of-attack on the local heat transfer distributions in short rectangular channels of narrow aspect ratios and identify the effect of 'crossed' ribs on heat transfer performance.

This investigation is a continuation of the work of refs. [3, 4]. The objective was to study the combined effects of the channel aspect ratio and the rib angle-

NOMENCLATURE

A heat transfer surface area
a plenum width
b plenum height
CR contraction ratio between plenum and test channel, $ab/(WH)$
D channel hydraulic diameter, $2WH/(W+H)$
e rib height
e^+ roughness Reynolds number, $(e/D)Re(f/2)^{1/2}$
f friction factor for four-sided ribbed channel
$\bar{f}$ average friction factor in a channel with two opposite ribbed walls
f(FD) fully developed smooth tube friction factor; also friction factor for four-sided smooth channel
G mass flux, $\rho\bar{V}$; also heat transfer roughness function
g_c conversion factor
H flow channel height
h heat transfer coefficient
K thermal conductivity of air
ΔL channel length for frictional pressure drop measurement
L test channel length
l plenum length
Nu Nusselt number, hD/K
Nu(FD) fully developed smooth tube Nusselt number; also Nusselt number for four-sided smooth channel
Nu_r ribbed side wall centerline-average Nusselt number for flow in a channel with two opposite ribbed walls
Nu_s smooth side wall centerline-average Nusselt number for flow in a channel with two opposite ribbed walls
ΔP pressure drop across the test section
P rib pitch
Pr Prandtl number of air
R friction roughness function
Re Reynolds number, GD/μ
St Stanton number, $Nu/(Re\ Pr)$, for flow in a channel with four-sided ribbed walls
St_r ribbed side wall centerline-average Stanton number for flow in a channel with two opposite ribbed walls
St_s smooth side wall centerline-average Stanton number for flow in a channel with two opposite ribbed walls
St(FD) fully developed smooth tube Stanton number; also Stanton number for four-sided smooth channel
$\overline{St}$ average of the centerline-average Stanton number for flow in a channel with two opposite ribbed walls
T_b bulk mean temperature of air
T_w local wall temperature
$\bar{V}$ average velocity of air
W flow channel width
W/H channel aspect ratio, ribs on side W
X axial distance from the heated test channel.

Greek symbols
α rib angle-of-attack
μ average viscosity of air
ρ average density of air.

of-attack on the local heat transfer distributions in short rectangular channels of small aspect ratios with a pair of opposite walls augmented by rib turbulators for Reynolds numbers from 10000 to 60000. The channel width-to-height ratios (W/H, ribs on side W) were 2/4 and 1/4. The channel length-to-hydraulic diameter ratios (L/D) were 10 and 15. In each channel, the brass ribs with a square cross section were glued periodically to the two opposite walls of the foil-heated channel so that the rib turbulators on opposite walls were parallel with an angle-of-attack of 90°, 60°, 45°, or 30°. The effect of crossed ribs was examined in the rectangular channel with $W/H = 2/4$ and with $\alpha = 60°$. The rib height-to-hydraulic diameter ratios (e/D) were 0.047 and 0.078; the rib pitch-to-height ratios (P/e) were 10 and 7.5. The local heat transfer distributions on both the rib-roughened side (side W) and the smooth side (side H) walls from the channel entrance to the downstream region were determined. The local heat transfer data after $X/D > 3$ were averaged and correlated, based on the heat transfer and friction similarity laws, to account for channel aspect ratio, rib height, rib angle, and Reynolds number. The highest heat transfer coefficient accompanied by the highest pressure drop and the best heat transfer performance for a constant pumping power were identified for rectangular channels with aspect ratios less than one.

EXPERIMENTAL PROGRAM

Foil heated test channel

The sketch and dimensions of the test channels are shown in Fig. 2(a) and Table 1. Two rectangular channels with small aspect ratios were fabricated. The first has a 5.1 cm × 10.2 cm (2 in. × 4 in.) cross section ($W/H = 2/4$); the second has a 2.55 cm × 10.2 cm (1 in. × 4 in.) cross section ($W/H = 1/4$). A plexiglas plenum was connected to the inlet of the test channel to provide a sudden entrance condition (entrance

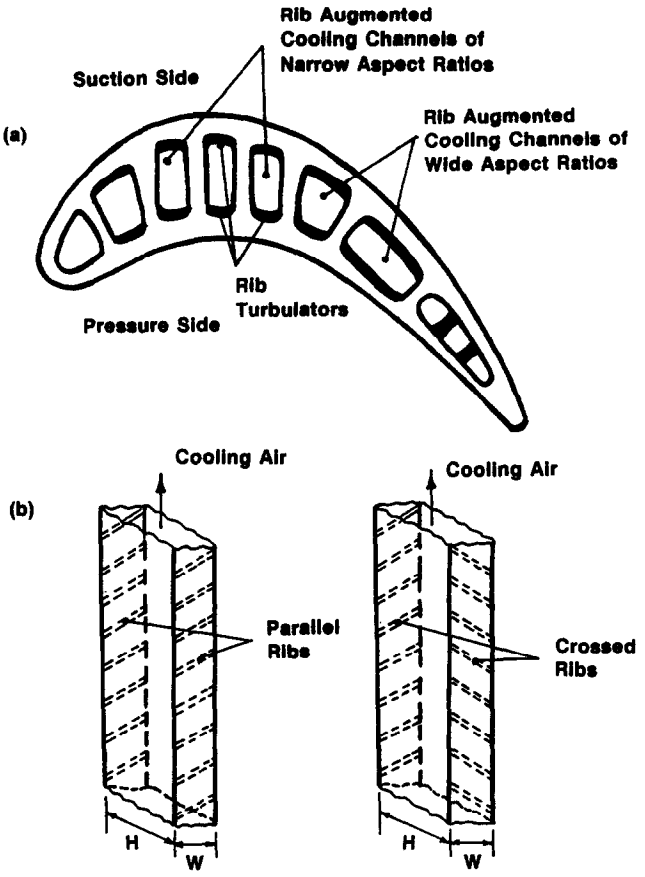

FIG. 1. (a) Cross-section of an internally-cooled turbine airfoil. (b) Rectangular channels of narrow aspect ratios with a pair of opposite rib-roughened walls (parallel ribs or crossed ribs).

developing flow). After the test channel, the air was exhausted into the atmosphere.

The rectangular channel consisted of four wood–plexiglas plates, each 1.92 cm (0.75 in.) thick. The 0.0025 cm (0.001 in.) thick, stainless steel foils were cemented separately to the inner face of each plate, controlled individually by a variac transformer for uniform electrical heating to the test channel, as shown in Fig. 2(b).

In each rectangular channel, the brass ribs of a square cross section were glued periodically on the left- and right-hand side plates of the foil-heated channels so that the ribs on opposite walls (side W) were parallel (or crossed) with a specified distribution. The thin layer of glue (<0.01 cm thick) ensured electrical isolation (but thermal conduction) from foil to brass ribs. The rib configurations for each test channel are shown in Fig. 2(c) and Table 2.

Thermocouple locations in each test channel are shown in Fig. 3. Each test channel has 100, 36 gauge, copper–constantan thermocouples soldered underneath the foils in strategic locations to measure the local surface temperature. The thermocouple locations were fixed although the rib angle α was varied from 90° to 30°. A Fluke 2280A Data Logger was interfaced to an IBM XT PC for data acquisition.

Data reduction

Six pressure taps along the centerline of the left-hand side ribbed wall and six along the centerline of the top smooth wall were used for static pressure drop measurements by a Dywer Microtector with an accuracy up to 0.025 mm (0.001 in.) of water. The pressure drop across the test channel was based on the isothermal conditions (tests without heating). The friction factor was calculated as

$$f = \Delta P/\{4(\Delta L/D)[G^2/(2\rho g_c)]\}. \quad (1)$$

Equation (1) was for the ribbed side wall and the smooth side wall friction factor calculations. The maximum uncertainty in the friction factor was estimated to be less than 9% for Reynolds numbers greater than 10 000. The friction factor of the present study was normalized by the friction factor for fully developed turbulent flow in smooth circular tubes ($10^4 < Re < 10^6$) proposed by Blasius as

$$f/f(\mathrm{FD}) = f/[0.046Re^{-0.2}]. \quad (2)$$

The local Nusselt number was calculated as

$$Nu = \{(q - q_{\mathrm{loss}})/[A(T_w - T_b)]\}\,(D/K). \quad (3)$$

Equation (3) was for the ribbed side wall and the

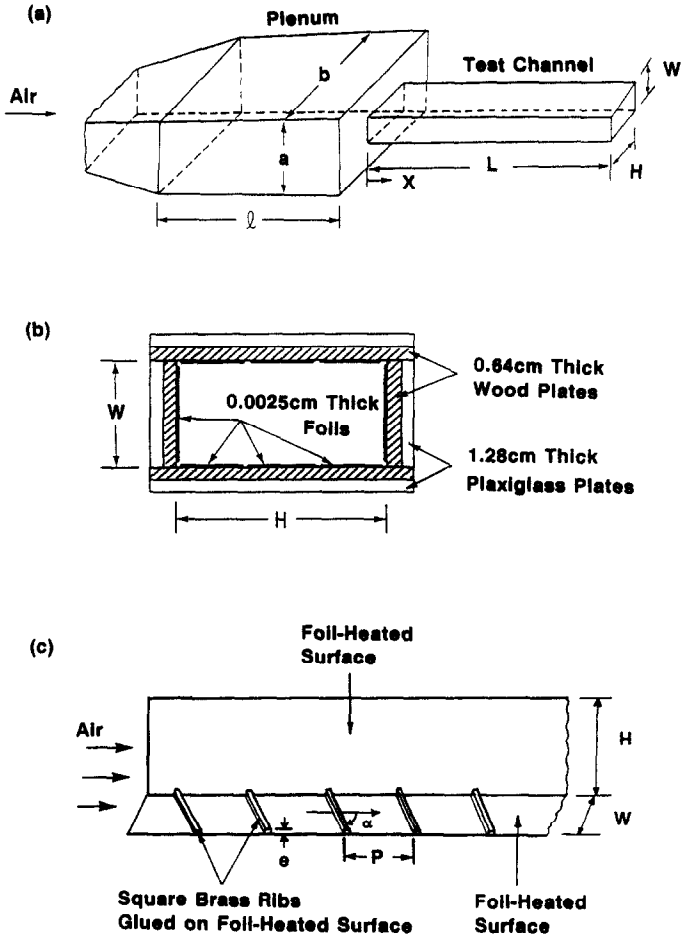

FIG. 2. (a) Sketch of the test channels and the inlet plenums. (b) Cross section of foil heated test channel. (c) Rib geometry in the test channel.

smooth side wall Nusselt number calculations. The local net heat transfer rate was the electrical power generated from the foil (q), minus the heat loss to the outside of the test channel (q_{loss}). The electric heat generation rate from the foil was determined from the measured foil resistance and the current through the foil on each surface. The effect of the local foil temperature variation on the local foil heat generation was estimated to be very small and negligible in calculations. The foil ensured a nearly uniform heat flux on each surface of the test channel. The maximum heat loss from the ribbed side wall and the smooth side wall was estimated to be less than 3 and 5%, respectively, for Reynolds numbers greater than 10000. To place the results on a common basis, the heat transfer area in equation (3) was always that of a smooth foil on each wall. The net heat flux level varied from 950 to 2500 W m^{-2} (300–800 BTU h^{-1} ft^{-2}) depending on the test conditions.

The local wall temperature in equation (3) was read from the thermocouple output. The local bulk mean air temperature in equation (3) was calculated from the measured inlet and outlet air temperatures, assuming a linear air temperature rise along the flow channel. The inlet bulk mean air temperature was 24–29°C (75–85°F) depending on the test conditions. The total net heat transfer rate from the test channel to the cooling air agreed well with the cooling air energy

Table 1. Dimensions of the test channels and the inlet plenums. Unit: cm

W	H	W/H	D	L	b	a	CR	l
5.1	10.2	2/4	6.8	127.5	30.6	15.3	9	15D
2.55	10.2	1/4	4.08	127.5	30.6	15.3	18	25D

Table 2. Rib geometries in each test channel. Unit: cm

W/H	Orientation	e	e/D	P/e	α
2/4	parallel ribs	0.32	0.047	10	90°, 60° 45°, 30°
2/4	parallel ribs	0.32	0.047	7.5	60°
2/4	crossed ribs	0.32	0.047	10	60°
1/4	parallel ribs	0.32	0.078	10	90°, 60° 45°

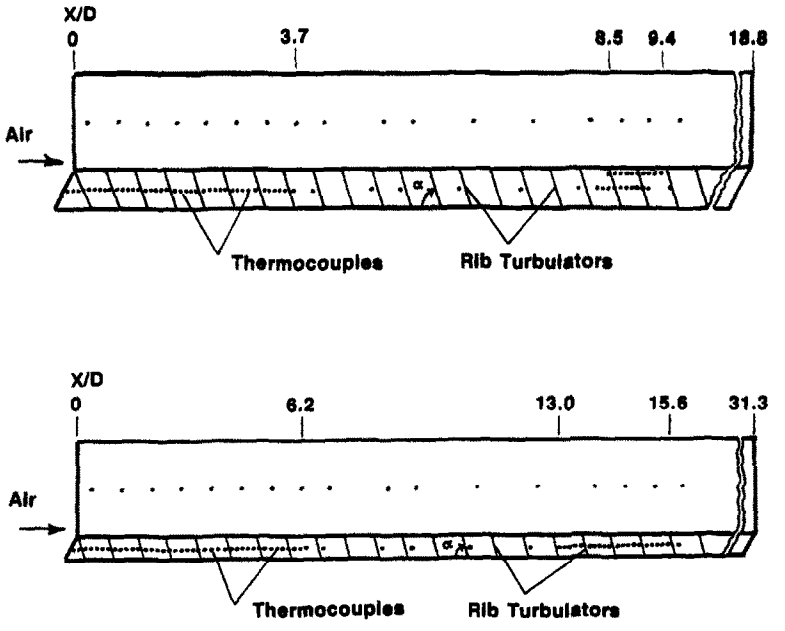

FIG. 3. Detailed thermocouple locations in each test channel.

rise along the test channel. The maximum uncertainty in the Nusselt number was estimated to be less than 8% for Reynolds numbers greater than 10 000. The local Nusselt number of the present study was normalized by the Nusselt number for fully developed turbulent flow in smooth circular tubes proposed by McAdams as

$$Nu/Nu(\mathrm{FD}) = Nu/(0.023Re^{0.8}Pr^{0.4}). \quad (4)$$

EXPERIMENTAL RESULTS AND DISCUSSION

The test results for the heat transfer coefficient and the friction factor in the smooth rectangular channels are given in ref. [5]. The maximum deviation of the Nusselt number from the McAdams correlation is 10%, and that of the friction factor from the Blasius equation is 12%.

The test results for ribbed channels are presented here. Twenty-seven runs (9 geometry by 3 Reynolds number) of local heat transfer data were obtained, as indicated in Table 2. The local heat transfer results are presented as the axial (streamwise) distributions of a normalized Nusselt number ratio, $Nu/Nu(\mathrm{FD})$, as given in equation (4). The local Nusselt number ratios along the centerlines of the ribbed side and the smooth side walls are not evenly distributed. In regions of interest, such as the entrance and the fully developed, the local Nusselt number was measured at up to five locations every rib pitch along the axial line, as indicated in Fig. 3. In regions between the entrance and the fully developed, the local Nusselt number was determined at only one location every rib pitch.

Local heat transfer coefficient: streamwise distribution

Effect of α and W/H. Typical results to illustrate the combined effects of the channel aspect ratio and the rib angle-of-attack on the centerline Nusselt number ratios are shown in Figs. 4 and 5 for parallel ribs with $P/e = 10$ and $Re = 30\,000$. In general, the local heat transfer distributions on the ribbed side wall behave differently with respect to rib angles-of-attack. In both channels ($W/H = 2/4$ and $1/4$), the centerline Nusselt number ratios for $\alpha = 90°$ maintain about the same level of periodic distribution after $X/D > 2$. The periodic profile of the local Nusselt number ratio is caused by flow separation from ribs and flow reattachment between ribs. The periodic Nusselt number ratios for $\alpha = 60°$ and $45°$ increase after $X/D > 2$, indicating that, in both narrow aspect ratio channels, the centerline Nusselt number ratios after $X/D > 2$ for $\alpha = 60°$ and $45°$ are higher than those for $\alpha = 90°$, as shown in Figs. 4 and 5. The increase in heat transfer may be due to the secondary flow induced by the rib angle. But the effect of the rib angle on the Nusselt number ratios after $X/D > 2$ is gradually reduced by further decreasing the rib angle to 30°, as shown in Fig. 4. Note the similar trend of the rib angle effect for the square channel ($W/H = 1$); the effect disappeared for the wider aspect ratio channel ($W/H = 4$) as indicated in ref. [3]. This study shows that the rib angle effect is important for the narrow aspect ratio channels ($W/H = 2/4$ and $1/4$).

Effect of crossed ribs. Typical results to demonstrate the effect of rib orientations of two opposite walls on the centerline Nusselt number ratios are shown in Fig. 6 for $W/H = 2/4$, $P/e = 10$, $\alpha = 60°$, and $Re = 30\,000$. The crossed ribs enhance about the same amount of heat transfer as the parallel ribs, except in the

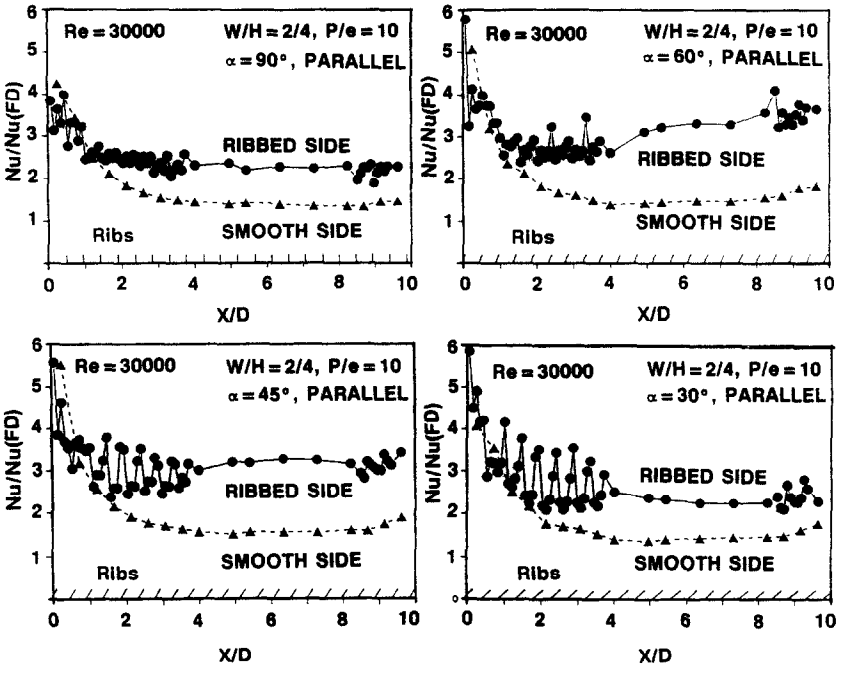

FIG. 4. The effect of rib angle on the centerline heat transfer distribution in a rectangular channel with $W/H = 2/4$.

downstream region where the enhancement is slightly reduced. The test results for $Re = 10000$ and 60000 show a similar trend; the heat transfer coefficients with opposite crossed ribs are slightly lower than those with opposite parallel ribs.

Effect of rib spacing. Typical results showing the effect of rib spacing on the centerline heat transfer coefficients are plotted in Fig. 7 for parallel ribs with $W/H = 2/4$, $\alpha = 60°$, and $Re = 30000$. For both $P/e = 10$ and 7.5, similar heat transfer patterns are observed, but the heat transfer coefficients for $P/e = 7.5$ are slightly higher than those for $P/e = 10$. This may be because $P/e = 7.5$ creates a shorter distance between flow reattachment, and flow hits the

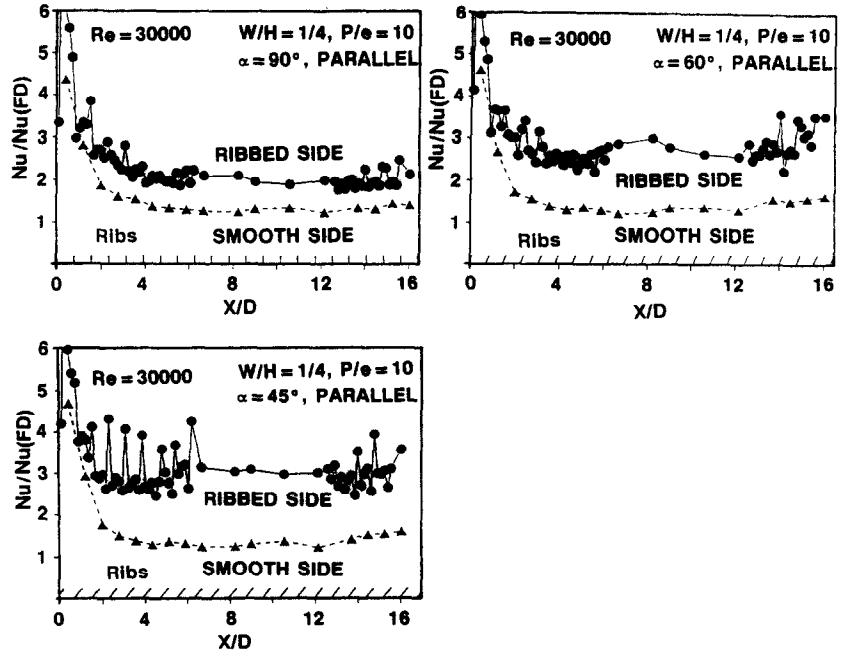

FIG. 5. The effect of rib angle on the centerline heat transfer distribution in a rectangular channel with $W/H = 1/4$.

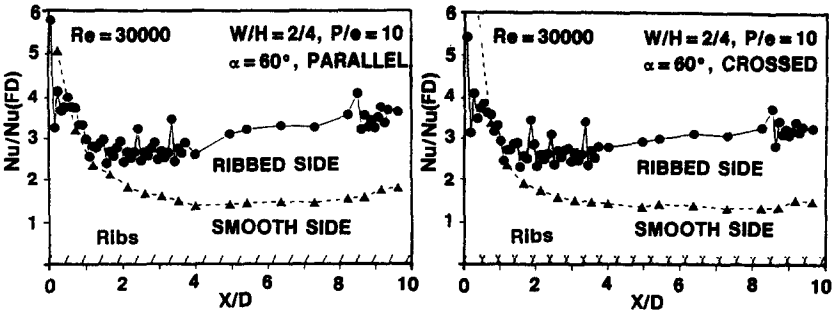

FIG. 6. The effect of crossed ribs on the centerline heat transfer distribution.

next rib. Also $P/e = 7.5$ adds more heat transfer surfaces from ribs than $P/e = 10$.

Local heat transfer coefficient: spanwise distribution

The streamwise-averaged Nusselt number ratio vs the spanwise (lateral) location is shown in Fig. 8 for $W/H = 2/4$, $P/e = 10$ and $Re = 30\,000$. The streamwise-averaged Nusselt number ratio is the average of the periodic Nusselt number ratios along the centerline and the edgeline, respectively, in the rectangular channel ($W/H = 2/4$) at the downstream region ($X/D = 8.5$–9.4). For $\alpha = 90°$, the streamwise-averaged Nusselt number ratio on the ribbed side wall is fairly uniform in the lateral direction as shown in Fig. 8. For $\alpha = 60°$, 45°, or 30°, the streamwise-averaged Nusselt number ratio on the ribbed side wall varies in the lateral direction; the Nusselt number ratio along the rib leading side is 20–30% higher than that along the centerline. This may be because the secondary flow moves along the rib axes from the left-hand side to the right-hand side. Therefore, the Nusselt number ratio on the rib leading side is higher than that in the centerline and subsequently should be higher than that on the rib trailing side (data were not taken). Also because of this secondary flow effect, the streamwise-averaged Nusselt number ratios with angled ribs are higher than those with transverse ribs.

Centerline average heat transfer and friction data

For $\alpha = 90°$, the local Nusselt number had a periodically developed distribution and the friction factor had a constant value after $X/D > 3$. Therefore, the heat transfer and friction data after $X/D > 3$ were used to obtain the average Nusselt number and the average friction factor, respectively. The ribbed side wall average Nusselt (or Stanton) number (Nu_r) and the smooth side wall average Nusselt (or Stanton) number (Nu_s) were based on the average value of the centerline Nusselt (or Stanton) number between $X/D = 2.9$–3.7 and 8.5–9.4 for the rectangular channel with $W/H = 2/4$, and between $X/D = 4.8$–6.2 and 13.0–15.6 for the rectangular channel with $W/H = 1/4$. These centerline-averaged Nusselt (or Stanton) numbers were also used for heat transfer performance comparison and for correlations discussed in later sections.

Typical results to show the effect of the rib angle on the heat transfer ratio and on the friction factor ratio are plotted in Fig. 9 for $W/H = 2/4$ and 1/4. The Nusselt number ratios and the friction factor ratios (both the ribbed side wall and the smooth side wall) at $\alpha = 60°$ and 45° are higher than those at $\alpha = 90°$ and 30°. The augmented Nusselt number decreases with increasing Reynolds number, but the friction factor penalty increases with increasing Reynolds number. The results generally show trends similar to the data for the square channel ($W/H = 1$) in ref. [3].

Figure 10 shows the effects of crossed ribs and rib spacing on the Nusselt number ratio and on the friction factor ratio for $W/H = 2/4$ and $\alpha = 60°$. As expected, the augmented heat transfer decreases slightly with increasing Reynolds number and the pressure drop penalty increases with Reynolds number. The Nusselt number ratios in the case of

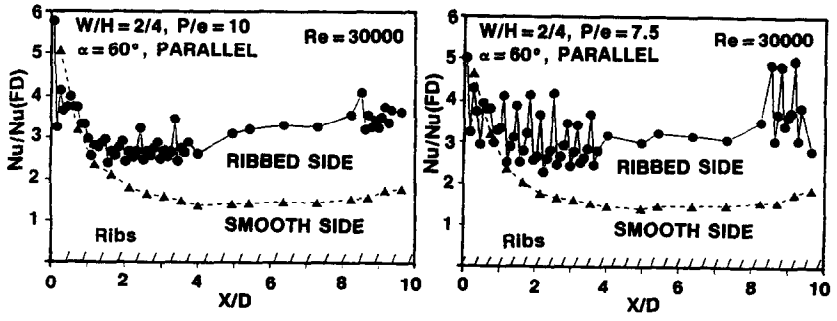

FIG. 7. The effect of rib spacing on the centerline heat transfer distribution.

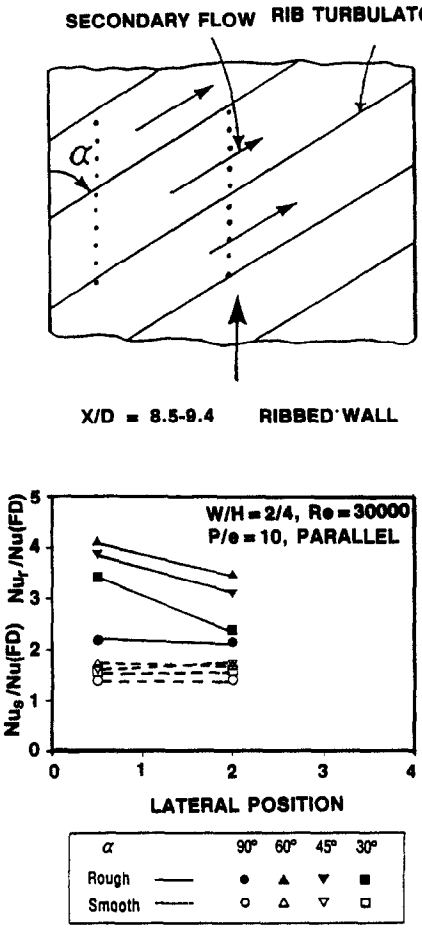

FIG. 8. The effect of rib angle on the lateral Nusselt number ratio.

crossed ribs are slightly lower than those of parallel ribs; both the Nusselt number and the friction factor ratios for $P/e = 7.5$ are slightly higher than for $P/e = 10$, as shown in Fig. 10.

Heat transfer performance comparison

As indicated in Figs. 9 and 10, the heat transfer augmentation in rib-roughened channels is always accompanied by the increased pressure drop through the same channels. One performance evaluation method for rib-roughened channels was comparison of the augmented ribbed-side-wall heat transfer, $St_r/St(\mathrm{FD})$, or the augmented average heat transfer, $\overline{St}/St(\mathrm{FD})$, for the same pumping power consumption through the flow channels, $[\bar{f}/f(\mathrm{FD})]^{1/3}$, as discussed in ref. [2]. Typical results to show the augmented heat transfer per pumping power vs roughness Reynolds number $[e^+ = (e/D)Re\sqrt{(f/2)}]$ are plotted in Fig. 11 for $W/H = 2/4$ and 1/4. The data of the square channel ($W/H = 2/2$, $e/D = 0.047$, and $P/e = 10$) from ref. [3] are included for comparison. The results show that both the highest ribbed side wall and the highest average heat transfer enhancements for a constant pumping power occur at $\alpha = 45°$ and then 60° for both narrow-aspect-ratio channels. But, both the highest ribbed side wall and the highest average heat transfer enhancements for a constant pumping power occur at $\alpha = 30°$ and then 45° for the square channel ($W/H = 2/2$). Figure 11 also indicates that the ribbed side wall heat transfer augmentation for narrow-aspect-ratio channels is higher than that for the square channel at a given e^+ and a given rib angle. But the average heat transfer augmentation for all three channels is about the same at a given e^+ and a given rib angle. Note that for wider-aspect-ratio channels ($W/H = 2$ and 4), the heat transfer enhancements are insensitive to the rib angle-of-attack and are much lower than those of the square channels, as presented in ref. [3]. Figure 12 shows that the augmented heat transfer for a constant pumping power in the case of parallel ribs is slightly better than that of crossed ribs; the enhanced heat transfer for a constant pumping power for $P/e = 7.5$ is slightly higher than that of $P/e = 10$.

Heat transfer and friction correlations

Analytical methods predicting the heat transfer coefficients and the friction in rib-roughened channels are not available because of the complex flow field created by rib turbulators. Therefore heat transfer designers still rely on semi-empirical correlations over a range of rib configuration and flow Reynolds number of the heat transfer and the pressure drop calculations. Those semi-empirical correlations are derived from the law of the wall similarity and the heat and momentum transfer analogy for flow over a rough surface [6–12].

Based on the law of the wall similarity analysis, correlation of the friction factor was obtained [3] for fully developed turbulent flow in rectangular channels of wider aspect ratios ($W/H = 1$, 2, and 4). To apply the same analysis for fully developed turbulent flow in rectangular channels of narrower aspect ratios ($W/H = 2/4$ and 1/4) of the present study, the friction factor, the channel aspect ratio, and the rib height-to-hydraulic diameter ratio should be correlated into a so-called friction roughness function (R) for the geometrically similar roughness as

$$R = (2/f)^{1/2} + 2.5 \ln\{(2e/D)[2H/(W+H)]\} + 2.5 \quad (5)$$

where

$$f = \bar{f} + (H/W)[\bar{f} - f(\mathrm{FD})] \quad (6)$$

and $f(\mathrm{FD})$, the friction factor in smooth rectangular channels, can be calculated approximately from the Blasius equation for smooth circular tubes [1] as

$$f(\mathrm{FD}) = 0.046 Re^{-0.2}. \quad (7)$$

Correlation of the present friction data is shown in Fig. 13(a). Correlation of the square channel ($W/H = 2/2$) from ref. [3] is included for comparison.

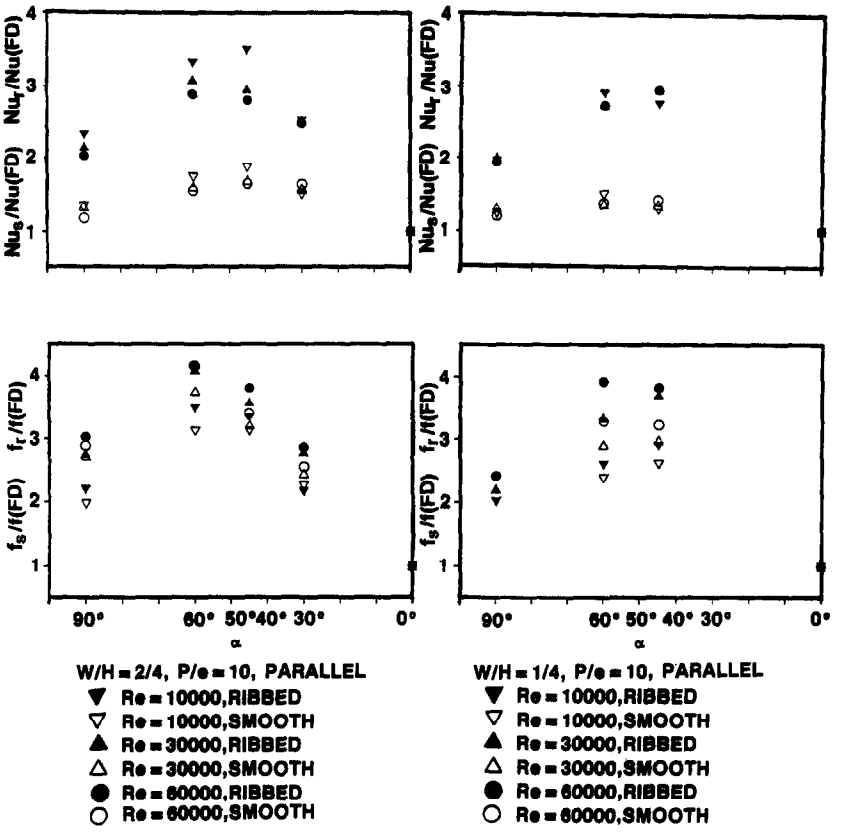

FIG. 9. Heat transfer and friction vs rib angle for $W/H = 2/4$ and 1/4.

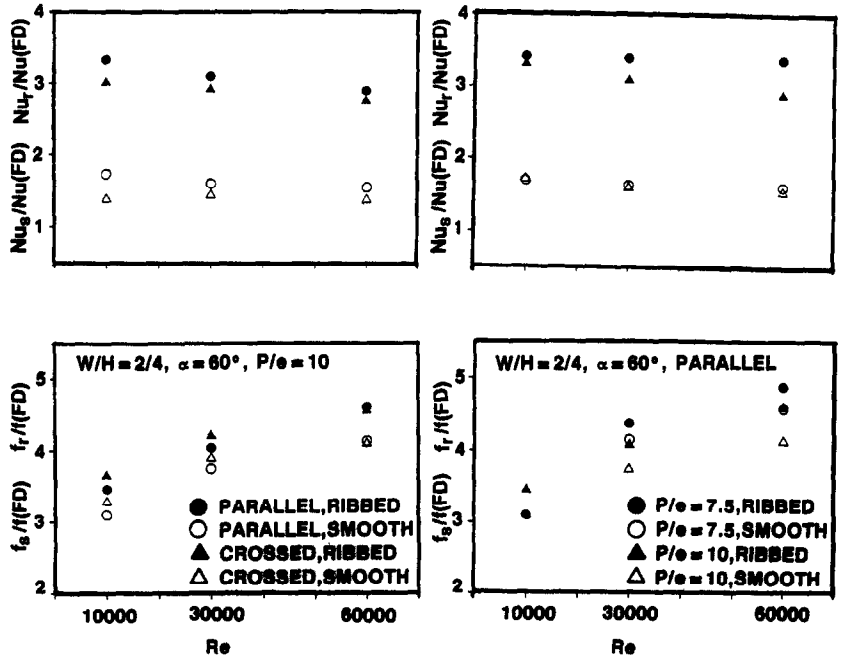

FIG. 10. Heat transfer and friction vs Reynolds number—effect of crossed ribs and rib spacing.

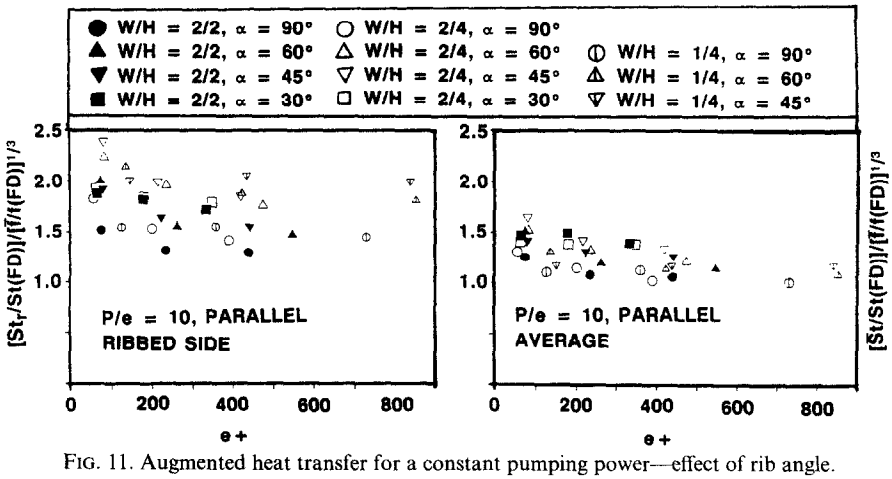

FIG. 11. Augmented heat transfer for a constant pumping power—effect of rib angle.

For a P/e of 10 of the present study, the dependence of R on α and W/H shown in Fig. 13(a) is

$$R = [12.31 - 27.07(\alpha/90°) + 17.86(\alpha/90°)^2](W/H)^m \quad (8)$$

where

$$m = -0.5, \qquad 60° \leqslant \alpha \leqslant 90°$$

$$m = -0.5(\alpha/60°)^2, \qquad 30° < \alpha < 60°$$

$$m = 0, \qquad \alpha \leqslant 30°.$$

The deviation of equation (8) is $\pm 6\%$ (except for 2 out of 21 data points). Note that R in equation (8) is independent of Reynolds number. After R is correlated experimentally from equation (8), the average friction factor ($\bar{f}$) of the present cooling channels with two opposite ribbed walls can be predicted by combining equations (5)–(8) for a given e/D, α, W/H, and Re, and by keeping $P/e = 10$.

Similarly, in rectangular channels of narrower aspect ratios ($W/H = 2/4$ and $1/4$) of the present study, the friction factor, the friction roughness function, and the ribbed side wall Stanton number (St_r) can be correlated into a so-called heat transfer roughness function (G) for the geometrically similar roughness as

$$G = R + [f/(2St_r) - 1]/(f/2)^{1/2}. \quad (9)$$

Correlation of the present heat transfer data is shown in Fig. 13(b). Correlation of the square channel ($W/H = 2/2$) from ref. [3] is included for comparison. For a Prandtl number of 0.7 of the present study, the dependence of G on α, W/H, and e^+ can be represented by

$$G = C(e^+)^n \quad (10)$$

where

for $2/4 \leqslant W/H \leqslant 1$,

$$n = 0.35$$
$$C = 2.24, \text{ if } \alpha = 90°$$
$$C = 1.80, \text{ if } 30° \leqslant \alpha < 90°$$

for $1/4 \leqslant W/H < 2/4$,

$$n = 0.35(W/H)^{0.44}$$
$$C = 2.24(W/H)^{-0.76}, \text{ if } \alpha = 90°$$
$$C = 1.80(W/H)^{-0.76}, \text{ if } 30° \leqslant \alpha < 90°.$$

The deviation of equation (10) is $\pm 8\%$ (except for 1 out of 21 data points). After G is correlated experimentally from equation (10), the ribbed side wall centerline-average Stanton number (St_r) can be

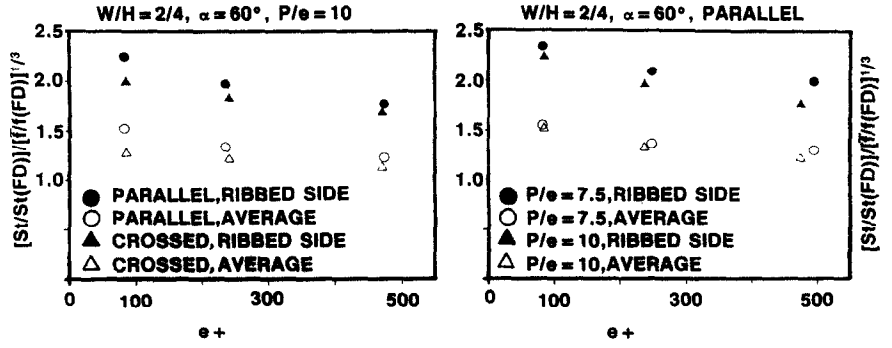

FIG. 12. Augmented heat transfer for a constant pumping power—effect of crossed ribs and rib spacing.

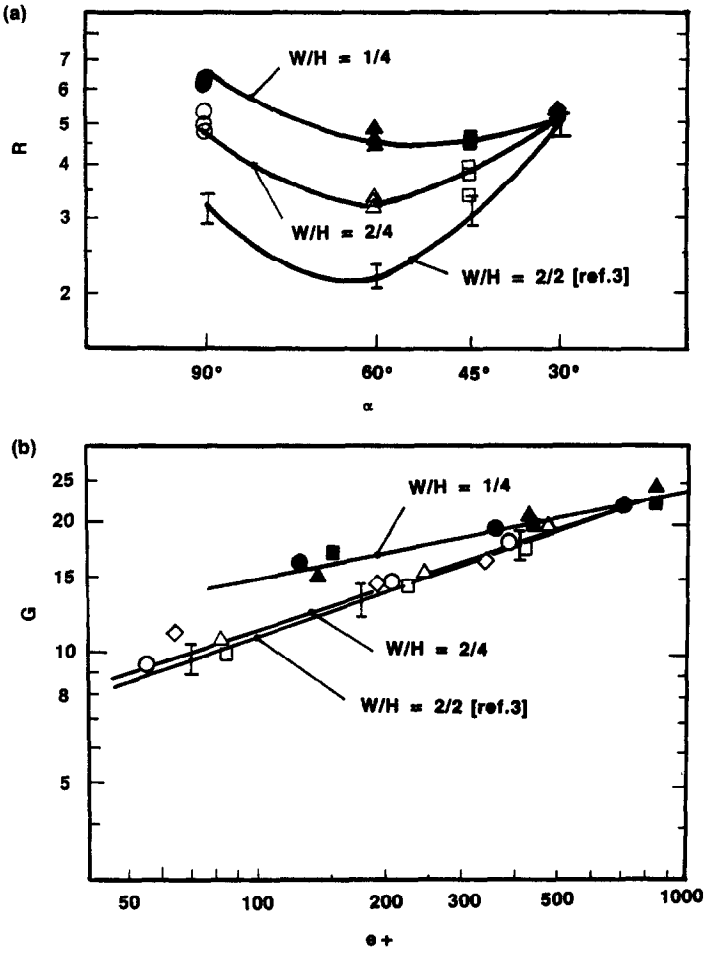

FIG. 13. (a) Friction correlation. (b) Heat transfer correlation.

predicted by combining equations (5), and (8)–(10) for a given e/D, α, W/H, and Re, and by keeping $P/e = 10$.

CONCLUDING REMARKS

The effects of the rib angle-of-attack on the distributions of the local heat transfer coefficient and on the friction factors in short rectangular channels of narrow aspect ratios ($W/H = 2/4$ and $1/4$) with two opposite rib-roughened walls have been studied. The main findings of the study are given below.

(1) For $\alpha = 90°$ or 30°, the local Nusselt number becomes uniformly periodic between ribs in the streamwise direction after several ribs from the channel entrance ($X/D > 3$); for $\alpha = 60°$ or 45°, the periodic Nusselt number increases in the steamwise direction after $X/D > 3$ because of the secondary flow induced by the rib angle.

(2) For $\alpha = 60°$, 45°, or 30°, after $X/D > 3$ the Nusselt number decreases monotonically along the rib axes (lateral) direction because of the secondary flow induced by the rib angle.

(3) For $W/H = 2/4$ and $1/4$, the highest heat transfer augmentation and the accompanying highest pressure drop penalty occur at $\alpha = 60°$ (and then 45°); the best heat transfer performance for a constant pumping power can be obtained at $\alpha = 45°$ (and then 60°); the ribbed-side-wall heat transfer performance with angled ribs ($\alpha = 60°$ and 45°) is about 25–35% higher than that with the transverse ribs ($\alpha = 90°$).

(4) The ribbed side wall heat transfer performance for narrow-aspect-ratio channels ($W/H = 2/4$, $1/4$) is better than that for the square channel at a given e^+ and rib angle. But the average heat transfer performance for all three channels is about the same at a given e^+ and rib angle. From ref. [3], the heat transfer performance for the square channel is much better than that for wide-aspect-ratio channels ($W/H = 2$ and 4).

(5) For $W/H = 2/4$, $P/e = 10$, and $\alpha = 60°$, the ribbed side wall heat transfer performance in the case of crossed ribs is slightly lower (5–10%) than that of parallel ribs for a constant pumping power; for $W/H = 2/4$ and $\alpha = 60°$, the $P/e = 7.5$ provides a 5–10% higher heat transfer performance of the ribbed side wall than the $P/e = 10$ for a constant pumping power.

(6) The friction and heat transfer correlations are developed to account for rib angle, channel aspect ratio, rib height, and Reynolds number. The correlations are valid for $e^+ \geqslant 50$, $30° \leqslant \alpha \leqslant 90°$, $0.047 \leqslant e/D \leqslant 0.078$, $1/4 \leqslant W/H \leqslant 1$, $10\,000 \leqslant Re \leqslant 60\,000$, and for $P/e = 10$. The correlations can be used in the design of advanced turbine cooling channels with narrow aspect ratios.

Acknowledgement—This work was funded by the NASA–Lewis Research Center under grant No. NAG 3-311 and contract No. NAS 3-24227. Very special thanks are due to Dr Robert Simoneau and Mr Robert Boyle of the NASA–Lewis Reserch Center for supporting and monitoring the project. The support of Mr Curtis Walker (deceased 1985) of the U.S. Army–Propulsion Laboratory and the efforts of Mr Francis Stepka (deceased 1982) of NASA–Lewis Research Center were invaluable to this project. This concluding report is dedicated to their memory.

REFERENCES

1. J. C. Han, Heat transfer and friction in channels with two opposite rib-roughened walls, *ASME J. Heat Transfer* **106,** 774–781 (1984).
2. J. C. Han, J. S. Park and C. K. Lei, Heat transfer enhancement in channels with turbulence promoters, *ASME J. Engng Gas Turbines Pwr* **107,** 628–635 (1985).
3. J. C. Han and J. S. Park, Developing heat transfer in rectangular channels with rib turbulators, *Int. J. Heat Mass Transfer* **31,** 183–195 (1988).
4. J. C. Han, Heat transfer and friction characteristics in rectangular channels with rib turbulators, *ASME J. Heat Transfer* **110,** 321–328 (1988).
5. J. C. Han, J. S. Park and M. Y. Ibrahim, Measurement of heat transfer and pressure drop in rectangular channels with turbulence promoters, NASA Contractor Report 4015 (or AVSCOM Technical Report 86-C-25), pp. 1–197 (1986).
6. J. Nikuradse, Laws for flow in rough pipe, NACA TM 1292 (1950).
7. D. F. Dipprey and R. H. Sabersky, Heat and momentum transfer in smooth and rough tubes in various Prandtl number, *Int. J. Heat Mass Transfer* **6,** 329–353 (1963).
8. R. L. Webb, E. R. G. Eckert and R. J. Goldstein, Heat transfer and friction in tubes with repeated-rib roughness, *Int. J. Heat Mass Transfer* **14,** 601–617 (1971).
9. M. Dalle Done and L. Meyer, Turbulent convective heat transfer from rough surfaces with two-dimensional rectangular ribs, *Int. J. Heat Mass Transfer* **20,** 582–620 (1977).
10. J. C. Han, L. R. Glicksman and W. M. Rohsenow, An investigation of heat transfer and friction for rib-roughened surfaces, *Int. J. Heat Mass Transfer* **21,** 1143–1156 (1978).
11. D. L. Gee and R. L. Webb, Forced convection heat transfer in helically rib-roughened tubes, *Int. J. Heat Mass Transfer* **23,** 1127–1136 (1980).
12. R. Sethumadhavan and M. Raja Rao, Turbulent flow heat transfer and fluid friction in helical-wire-coil-inserted tubes, *Int. J. Heat Mass Transfer* **26,** 1833–1844 (1983).

ACCROISSEMENT DU TRANSFERT DE CHALEUR DANS DES CANAUX RECTANGULAIRES A FAIBLE RAPPORT DE FORME AVEC DES NERVURES TURBULATRICES

Résumé—Les effets de l'angle d'attaque des nervures sur les distributions du coefficient local de transfert thermique et sur les coefficients de frottement dans des canaux rectangulaires courts, avec des faibles rapports de forme et avec une paire de parois opposées munies de nervures, sont déterminés pour des nombres de Reynolds entre 10 000 et 60 000; les rapports largeur/hauteur du canal sont 2/4 et 1/4; les angles d'attaque des nervures sont 90°, 60°, 45° et 30°. Les résultats montrent que les canaux à faible rapport de forme correspondent à une meilleure performance de transfert de chaleur pour une puissance égale de pompage. On obtient des formules semi-empiriques pour le frottement et le transfert thermique. Les résultats peuvent être utilisés dans la conception des canaux à faible rapport de forme, pour le refroidissement des turbines.

VERBESSERUNG DES WÄRMEÜBERGANGS IN BERIPPTEN RECHTECKKANÄLEN

Zusammenfassung—Es wird der Einfluß der Rippenneigung auf die Verteilung des lokalen Wärmeübergangskoeffizienten und des Reibungsfaktors in kurzen engen Rechteckkanälen mit zwei sich gegenüberliegenden berippten Wänden für Reynolds-Zahlen von 10 000 bis 60 000 ermittelt. Untersucht werden Kanäle mit einem Breiten-Höhen-Verhältnis von 2/4 und 1/4 für Werte des Rippenneigungswinkels von 90°, 60°, 45° und 30°. Es zeigt sich, daß das Wärmeübertragungsverhalten bei konstanter Pumpenleistung in engen Kanälen besser ist als in weiten Kanälen. Es werden halbempirische Reibungs- und Wärmeübergangskorrelationen angegeben. Die Ergebnisse können bei der Auslegung von Kühlkanälen in Turbinen verwendet werden.

ИНТЕНСИФИЦИРОВАННЫЙ ТЕПЛОПЕРЕНОС В УЗКИХ ПРЯМОУГОЛЬНЫХ КАНАЛАХ С ТУРБУЛИЗАТОРАМИ В ВИДЕ РЕБЕР

Аннотация—При значениях числа Рейнольдса от 10 000 до 60 000 определено влияние угла атаки ребер на распределение локального коэффициента теплообмена и на коэффициенты трения в коротких узких прямоугольных каналах с оребрением двух противоположных стенок. Отношение ширины каналов к высоте равнялось 2/4 и 1/4; углы атаки ребер составляли соответственно 90°, 60°, 45° и 30°. Результаты показывают, что в узких каналах отмечается более эффективный перенос тепла, чем в широких при том же расходе жидкости. Получены полуэмпирические соотношения для учета трения и теплопереноса. Результаты могут использоваться при расчете узких каналов систем охлаждения турбин.